Applications of the Common-Reflection-Surface Stack

Jürgen Mann, Thilo Müller, Rainer Jäger, German Höcht, and Peter Hubral, Geophysical Institute, University of Karlsruhe, Germany*

Summary

The simulation of a zero-offset stack section from multi-coverage seismic reflection data for 2-D media is a widely used seismic reflection imaging method that reduces the amount of data and enhances the signal-to-noise ratio. The aim of the common-reflection-surface stack is not only to provide a well-simulated zero-offset stack section but also to determine certain attributes of hypothetical wavefronts at the surface useful for a subsequent inversion.

The main advantage of the common-reflection-surface stack is the use of analytical formulae that describe the kinematic reflection moveout response for inhomogeneous media with curved interfaces. These moveout formulae are valid for arbitrary shot-receiver pairs with respect to a common reference point and do not depend on the macro velocity model. An analytic reflection response that fits best to an actual reflection event in the multi-coverage data set is determined by coherency analysis.

We applied the common-reflection-surface stack to various synthetic and real data sets. For synthetic data sets, i. e. for a given model, data-derived as well as model-derived (forward calculated) wavefront attributes were computed. This enables us to verify the wavefront attributes determined by the common-reflection-surface stack exposing a wide agreement with the expected results. For real data sets we compare conventional stacking results and the common-reflection-surface stack.

Introduction

Many conventional imaging methods require a sufficiently accurate macro velocity model to yield correct results. To calculate the respective operators (e. g. the stacking trajectories for dip moveout (DMO) correction or traveltime surfaces associated with hypothetical diffractors for pre-stack migration (PSM)) it is in addition necessary to perform ray tracing to obtain the traveltimes.

Our aim is to determine appropriate 2-D stacking operators without the knowledge of a macro velocity model and, consequently, without ray tracing. This approach is based on ideas of de Bazelaire (1988) and Berkovitch et al. (1994).

The "best" stacking operator is determined by means of coherency analysis (Taner and Koehler, 1969): we test a set of different stacking operators for the highest coherence obtained along the respective operator in the input data set.

For homogeneous models the stacking operator is the kinematic multi-coverage response of a circular reflector segment in the subsurface, the *common reflection surface* (CRS). This response can be described by means of three parameters: the reflector segment's location, orientation, and curvature. Performing two hypothetical experiments with sources on the CRS yields wavefronts associated with two so-called *eigenwaves* (Hubral, 1983). These wavefronts would be observed at the surface with well-defined attributes, namely the angles of emergence (which coincide for both eigenwaves) and the respective curvatures of the two emerging hypothetical wavefronts. In other words, the common angle of emergence and the two curvatures uniquely define the considered three-parametric circular reflector segment and its multi-coverage reflection response.

Moving to the more general case of inhomogeneous models, these wavefront attributes can still be used to define the stacking operator assuming the emerging hypothetical wavefronts to be circular in a certain vicinity of the surface location under consideration.

Theory

The two hypothetical experiments providing the wavefronts of the eigenwaves are illustrated in Figures 1 and 2 for a model with three homogeneous layers. We consider a point R on the second interface associated with a normal incidence ray (shown as bold blue line) emerging at location x_0 on the surface.

One eigenwave is obtained by placing a point source at R that produces the so-called upgoing *normal incidence point* (*NIP*) wave (Figure 1, wavefronts depicted in blue). An exploding reflector experiment yields the second upgoing eigenwave called *normal* (*N*) wave. The wavefronts are again depicted in blue (Figure 2). In a vicinity of x_0 both wavefronts are approximated by circles with the radii of curvature R_{NIP} (shown in green) and R_N (shown in red), respectively.

The CRS stacking operator can be derived in different ways, e. g. according to the geometrical approach of Höcht (1998) which yields a parametric representation of the stacking operator. The parameters are the angle of emergence α of the normal incidence ray, the radius of curvature R_{NIP} of the *NIP* wave, and the radius of curvature R_N of the *normal* wave.

However, for irregular acquisition geometries an explicit representation of the stacking operator is more convenient. A hyperbolic second order Taylor expansion, which can also be derived by means of paraxial ray theory (Schleicher et al., 1993; Tygel et al., 1997), reads

$$\begin{aligned} t^2(x_m,h) &= \left(t_0 + \frac{2\sin\alpha}{v_0}(x_m - x_0)\right)^2 \\ &+ \frac{2t_0\cos^2\alpha}{v_0}\left(\frac{(x_m - x_0)^2}{R_N} + \frac{h^2}{R_{NIP}}\right) . \end{aligned}$$

The half-offset between source and receiver is denoted with h, whereas x_m denotes the midpoint between source and receiver. The only required model parameter is the near surface velocity

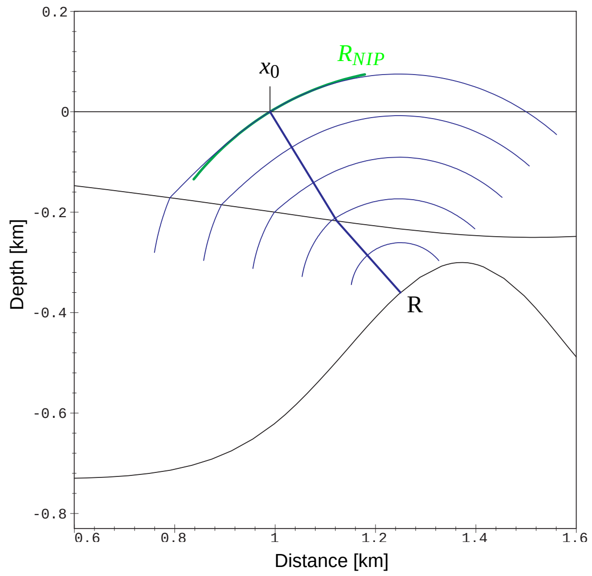

Fig. 1: Hypothetical experiment providing the *NIP* wave produced by a point source located at point R. The wavefronts are depicted in blue, the circular approximation in green. The normal incidence ray (bold blue line) is reflected at point R.

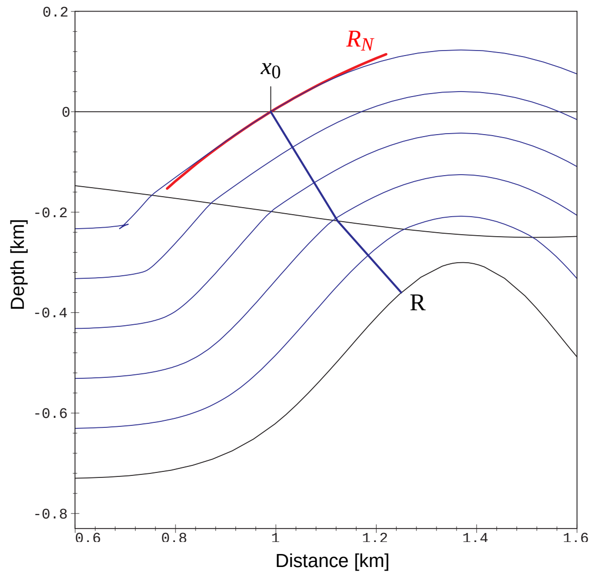

Fig. 2: Hypothetical experiment providing the *normal* wave generated by an exploding reflector experiment. The wavefronts are depicted in blue, the circular approximation in red. The normal incidence ray (bold blue line) is reflected at point R.

v_0. The respective sample of the ZO trace to be simulated is defined by (t_0, x_0).

According to Ursin (1982) and our own experience with different approximations of the CRS stacking operator the hyperbolic approximation of t^2 given above is more appropriate than a parabolic approximation of t (Schleicher et al., 1993). A double square root representation is also possible as shown by Berkovitch et al. (1994).

The proposed strategy can be applied to complex media. In the presented form it is based on ZO rays with normal incidence on the reflector. Furthermore, the CRS stacking operator is only valid in the vicinity of the ZO ray. With regard to ray theory this concerns the paraxial rays of the (central) ZO ray.

CRS Stack

For each sample (t_0, x_0) in the stack section, i. e. the zero-offset (ZO) section to be simulated, we have to determine the stacking parameter triple (α, R_{NIP}, R_N) that yields the stacking operator that fits best to an event in the multi-coverage data set. This is done by means of coherency analysis of the stacking operator with the measured data.

To avoid the time-consuming search for all three parameters at a time, three one-parametric searches are done. Firstly, a one-parametric search is performed to determine the squared stacking velocity $v_{NMO}^2 = 2\, v_0\, R_{NIP}/(t_0 \cos^2 \alpha)$ in the common midpoint (CMP) gathers. Secondly, the angle of emergence is scanned in the output section of the first search step (i. e. the CMP stacked section) in a first order approximation. Thirdly, in a second order approximation the radius of curvature R_N of the *normal* wave is been searched for. This yields all three parameters for each time sample. Wherever the coherence exceeds a given threshold an additional three-parametric optimization can be applied to improve the accuracy of the parameter triple. Finally, the measured data is summed up along the so-defined stacking operators to yield the CRS stacked section.

As a by-product, four additional output section are obtained. Each of the three stacking parameters as well as the coherency criterion in dependence of (t_0, x_0) are available. These parameter sections yield the potential for a subsequent inversion of the macro model.

Application

For a synthetic data set the CRS stacking method was successfully applied by Müller (1998). Since in this case the model is known, the exact stacking parameter can be forward calculated. By comparing the theoretical parameters with the ones determined by the CRS stacking method the accuracy of our approach has been tested. A comparison of model-derived versus data-derived parameters will be shown.

For a real data set the CRS stack was applied and compared to the result of the conventional processing chain NMO/DMO/stack. The results can be seen in Figures 3 and 4. The arrows in the CRS stack mark regions where the result differs substantially from the result of NMO/DMO/stack. The CRS stacking technique was able to image events that could not be seen in the NMO/DMO/stack. Generally, the image quality of the CRS stack is much better. The S/N ratio is increased and the continuity of the events is improved.

Let us emphasize once again that no other velocity information than the near surface velocity was used for the CRS stacking

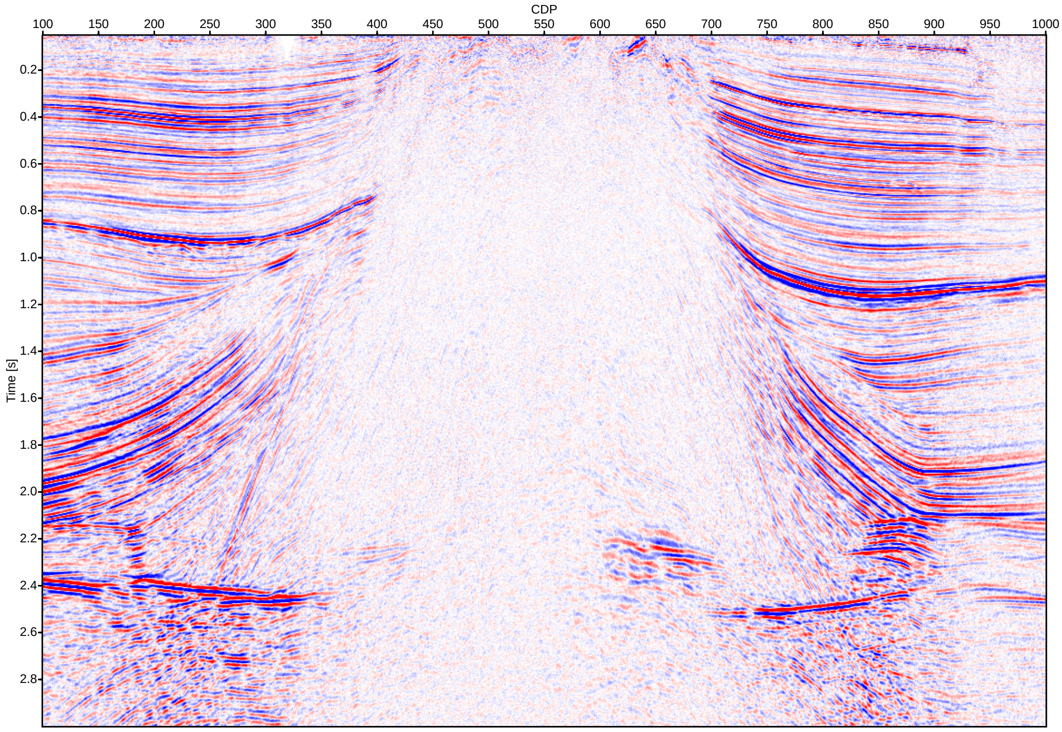

Fig. 3: Real data set: result of conventional NMO/DMO/stack.

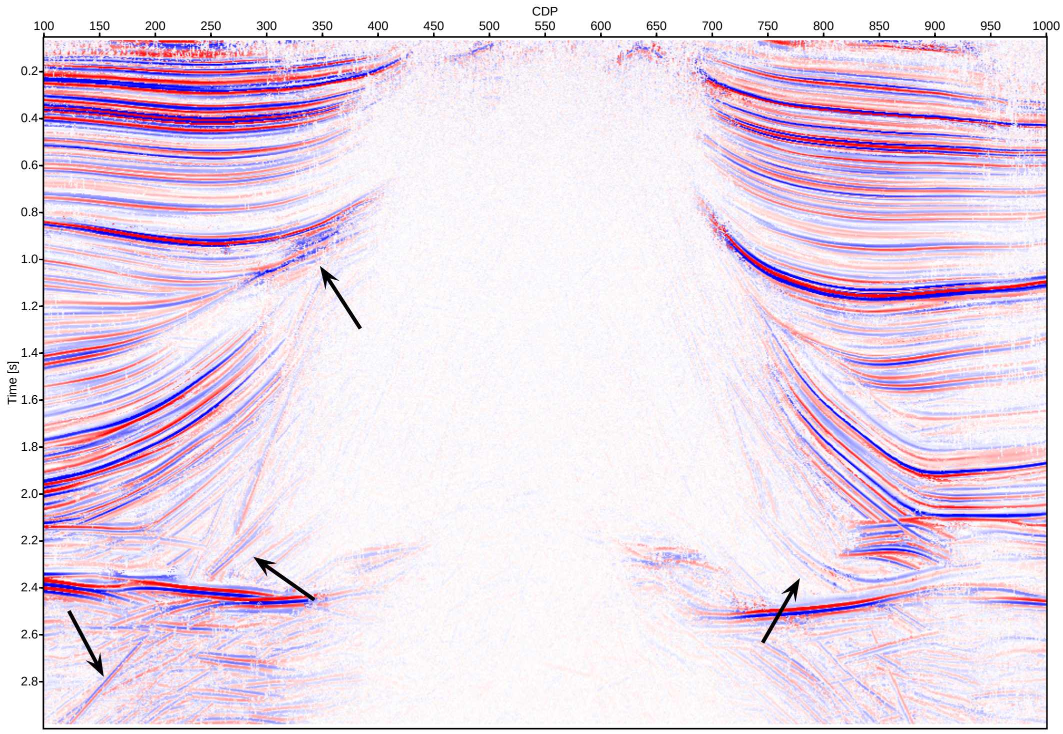

Fig. 4: Real data set: result of CRS stack. The major differences to the conventional stack are marked with arrows.

method, while for NMO/DMO/stack an intensive user-driven velocity analysis was needed.

Conclusions

The CRS stack is a model independent seismic imaging method and thereby can be performed without any ray tracing and macro velocity model estimation. Only the knowledge of the near surface velocity is required. As a result of a CRS stack one obtains in addition to each simulated ZO sample important wavefield attributes: the angle of emergence and the radii of curvature of the *NIP* and the *normal* wave. These attributes can subsequently be used to derive an approximation of the inhomogeneous 2-D macro velocity model (Hubral and Krey, 1980; Goldin, 1986) which allows to determine an image in the depth domain.

The CRS stack can be applied to traces on an arbitrarily irregular grid without the need of trace interpolation. Additionally, the simulated ZO section and the attribute sections are not restricted to the (possibly irregular) input data geometry.

The application of the CRS stack showed noteworthy results with respect to the stack section and the determined attributes. The real data example presented exposed significant differences in comparison to the result of NMO/DMO/stack. Namely, the continuity of the events and the S/N ratio are enhanced.

In view of the authors, the proposed strategies offer an exciting approach to improve the stack section and to allow for a subsequent inversion.

Acknowledgements

This work was kindly supported by the *Wave Inversion Technology Consortium*, Karlsruhe, Germany and *Elf Exploration Production*, Pau, France. We would like to thank *BEB Erdgas und Erdöl GmbH*, Hannover, Germany and *Preussag Energie GmbH*, Lingen, Germany for providing the data set and the permission to publish this work.

References

Berkovitch, A., Gelchinsky, B., and Keydar, S., 1994, Basic formulae for multifocusing stack: 56th Mtg. Eur. Assoc. Expl Geophys., Extended Abstracts, Session: P140.

de Bazelaire, E., and Thore, P., 1987, Pattern recognition applied to time and velocity contours: 57th Annual Internat. Mtg., Soc. Expl. Geophys., Expanded Abstracts, Session: POS2.14.

de Bazelaire, E., 1988, Normal moveout revisited – inhomogeneous media and curved interfaces: Geophysics, **53**, no. 2, 143–157.

Goldin, S. V., 1986, Seismic traveltime inversion: Soc. Expl. Geophys., Tulsa.

Höcht, G., 1998, Common reflection surface stack: Master's thesis, Universität Karlsruhe (GER).

Hubral, P., and Krey, T., 1980, Interval velocities from seismic reflection traveltime measurements *: Soc. Expl. Geophys.

Hubral, P., 1983, Computing true amplitude reflections in a laterally inhomogeneous earth: Geophysics, **48**, no. 8, 1051–1062.

Müller, T., 1998, Common Reflection Surface Stack versus NMO/STACK and NMO/DMO/STACK: 60th Mtg. Eur. Assoc. Expl Geophys., Extended Abstracts, 1–20.

Schleicher, J., Tygel, M., and Hubral, P., 1993, Parabolic and hyperbolic paraxial two-point traveltimes in 3D media: Geophys. Prosp., **41**, no. 4, 459–513.

Taner, M. T., and Koehler, F., 1969, Velocity spectra – digital computer derivation and applications of velocity functions *: Geophysics, **34**, no. 6, 859–881.

Tygel, M., Müller, T., Hubral, P., and Schleicher, J., 1997, Eigenwave based multiparameter traveltime expansions: 67th Annual Internat. Mtg., Soc. Expl. Geophys., Expanded Abstracts, 1770–1773.

Ursin, B., 1982, Quadratic wavefront and traveltime approximations in inhomogeneous layered media with curved interfaces: Geophysics, **47**, no. 7, 1012–1021.